PCCP

Accepted Manuscript

ROYAL SOCIETY OF CHEMISTRY

www.rsc.org/pccp

A look into amyloid formation by transthyretin: aggregation pathway and a novel kinetic model

Tiago Q. Faria[1,*,§], Zaida L. de Almeida[1,§], Pedro F. Cruz[2], Catarina S. H. Jesus[1,2], Pedro Castanheira[3], Rui M. M. Brito[1,2,*]

[1]Center for Neuroscience and Cell Biology, University of Coimbra, Coimbra, Portugal
[2]Chemistry Department, University of Coimbra, Coimbra, Portugal
[3]Biocant – Biotechnology Innovation Center, Parque Tecnológico de Cantanhede, Cantanhede, Portugal

[§] Tiago Q. Faria and Zaida L. de Almeida contributed equally to this work.

*Corresponding authors
Correspondence may be addressed to either of these authors:
Tiago Q. Faria: tfaria@qui.uc.pt
Rui M. M. Brito: brito@ci.uc.pt

ABSTRACT

The aggregation of proteins into insoluble amyloid fibrils is the hallmark of many, highly debilitating, human pathologies as Alzheimer's or Parkinson's diseases. Transthyretin (TTR) is a homotetrameric protein implicated in several amyloidoses like Senile Systemic Amyloidosis (SSA), Familial Amyloid Polyneuropathy (FAP), Familial Amyloid Cardiomyopathy (FAC), and the rare Central Nervous System selective Amyloidosis (CNSA). In this work, we have investigated the kinetics of TTR aggregation into amyloid fibrils produced by the addition of NaCl to acid-unfolded TTR monomers and we propose a mathematically simple kinetic mechanism to analyse the aggregation kinetics of TTR. We have used circular dichroism, intrinsic tryptophan fluorescence and thioflavin-T emission to follow the conformational changes accompanying amyloid formation at different TTR concentrations. Kinetic traces were adjusted to a two-step model with the first step being second-order and the second being unimolecular. The molecular species present in the pathway of TTR oligomerization were characterized by size exclusion chromatography coupled to a multi-angle light scattering apparatus and by transmission electron microscopy. The results show the transient accumulation of oligomers composed by 6 to 10 monomers in agreement with reports suggesting that these oligomers may be the causative agent of cell toxicity. The results obtained may prove useful in the understanding of the mode of action of compounds able to prevent fibril formation and, therefore, in designing new drugs against TTR amyloidosis.

ABBREVIATIONS

TTR: transthyretin; CD: circular dichroism; ThT: Thioflavin-T; SEC: size exclusion chromatography; MALS: multi-angle light scattering; TEM: transmission electron microscopy; NMR: Nuclear magnetic resonance; HMQC: Heteronuclear multiple-quantum correlation.

INTRODUCTION

The aggregation of proteins is implicated in many, highly debilitating, human pathologies and, additionally, it is a crucial aspect in the production, purification and storage of proteins for industrial applications affecting their yields and efficacy.[1,2] In

amyloidogenic diseases such as Alzheimer's, Spongiform Encephalophaties, Parkinson's and Familial Amyloid Polyneuropathy (FAP), normally soluble peptides or proteins undergo conformational changes and aggregate into insoluble and highly stable amyloid fibrils. To date, more than forty different human peptides and proteins, like amyloid-β peptide, prion protein, α-synuclein and transthyretin (TTR), have been identified in disease-associated amyloid deposits which are responsible for the above mentioned amyloidoses.[3-5]

No sequence, structural or functional correlations are apparent among many of the proteins that display the ability to form amyloid. Despite these dissimilarities, amyloid fibrils from different sources share many common structural features forming long, straight, unbranched filaments with a cross-β sheet conformation with the β-strands oriented perpendicularly to the fibril main axis. Often, mature fibrils also reveal a periodic structure due to the twist of multiple protofilaments around each other.[4-7] Amyloid fibrils have, as well, identical tinctorial properties being able to bind Congo Red or Thioflavin-T (ThT) dyes among others.[8,9] In spite of many structural similarities, recent studies show that at a molecular level, packed amyloid proteins can adopt distinct conformations that may play a relevant role on the phenotype of different pathologies caused by the same protein.[10,11]

Fibrillar structures formed by the protein TTR are implicated in several amyloidosis.[3,12] In Senile Systemic Amyloidosis (SSA) fibrils are derived from wild-type TTR and this pathology is characterized by amyloid deposition in the heart leading to congestive heart failure. Typically presents itself after age 60, affecting as much as 25 % of the population over the age of 80.[13] Familial Amyloid Polyneuropathy (FAP),[14,15] Familial Amyloid Cardiomyopathy (FAC),[16] and the rare Central Nervous System selective Amyloidosis (CNSA)[17,18] are pathologies caused by different TTR variants and they depend on the organ(s) and/or tissue(s) affected by amyloid deposition: peripheral nerves, heart, and leptomeninges and subarachnoid vessels, respectively. The age of onset varies from 20 to 70 years with a mean age of onset in the 30s in the FAP Portuguese cohort, while in FAC the age of onset is similar to that in SSA. Around 100 mutations have been found to date in TTR, many of them amyloidogenic.[3,12,19] Physiologically, TTR is mainly synthesized in the liver, the choroid plexus, and the retina of the eye, and it is found in plasma, cerebrospinal fluid and the eye among other tissues. TTR has two identical thyroxine-binding sites serving as a transport protein for

this hormone and is also involved in the transport of retinol in association with the retinol-binding protein.[3,20,21]

In structural terms, TTR is a homotetrameric protein with a total molecular mass of 55 kDa. Each monomeric subunit is composed of a β-sandwich of two four-stranded β-sheets. The subunits dimerize by intermolecular antiparallel β-sheet formation yielding an eight-stranded β-sandwich and the two dimers interact to form a tetramer through hydrophobic interactions and hydrogen bonds.[20-23] Several studies on the aggregation pathway of TTR demonstrate that TTR amyloid fibril formation is preceded by the dissociation of the native tetramer to non-native monomeric species that can self-assemble into non-fibrillar and cytotoxic oligomers which are prone to form protofibrils and further elongate into mature amyloid fibrils.[24-28]

Due to its clinical implications, the aggregation of proteins has been a subject of large scientific interest and several models have been put forward to analyze the kinetics and mechanism of protein amyloidosis.[1,2] Quantitative understanding of the kinetics of fibril formation will lead to a better understanding of the factors that influence the propensity for protein aggregation into amyloid fibrils. In addition, knowledge of the molecular mechanisms involved in the cascade of events underlying protein self-assembly should lead to strategies useful to prevent or control amyloid formation and to contribute to the design of small-molecule drugs that can inhibit a given kinetic step.[29]

Several mathematical methods are reported in the literature to analyze kinetic data of amyloid formation.[1,2] Typically, aggregation models are composed of two main steps: nucleation and growth. In cases where nucleation is the rate limiting step, a lag-phase is usually observed corresponding to the time required for the formation of a thermodynamic nucleus which is the species with the highest energy along the assembly reaction. This lag-phase can be by-passed by adding preformed aggregates (or seeds) to the reaction mixture. Most of the mathematical models to fit these kinetic data make assumptions only valid for the classic nucleation-growth reactions where the first step is much slower than the second one. This is not the case for TTR amyloidogenesis where no lag phase is observed.[30,31] Recently, a simple model based on the fundamentals of crystal growth was proposed.[32] The authors claim that this crystallization-like model (CLM) is a generic model that can be used to analyze sigmoidal (classic nucleation-growth reactions presenting a lag-phase) and hyperbolic (traces without lag-phase) kinetic data. This two parameter model determines the magnitude of the growth step and the nucleation-to-growth magnitude as a function of protein supersaturation.

In this work, we characterized the kinetics of amyloid formation by TTR using circular dichroism (CD) and intrinsic tryptophan fluorescence to follow the TTR conformational changes accompanying amyloid formation. Additionally, ThT binding assays were used to monitor the time course of TTR oligomerization. In order to separate the initial process of tetramer dissociation from the oligomerization pathway, TTR assembly was triggered by the addition of salt to acid-unfolded TTR monomers.[28] Aiming at a better characterization of the molecular species present in the TTR oligomerization pathway, we have used size exclusion chromatography coupled to a multi-angle light scattering (SEC-MALS) apparatus and also transmission electron microscopy (TEM).

RESULTS

Acid-unfolded TTR

Extensive dialysis of native tetrameric TTR against 10 mM HCl, pH 2, leads to TTR tetramer dissociation and monomer unfolding originating a polypeptide chain with no significant secondary structure.[24,28] Upon unfolding, the minimum of the CD spectrum shifts from 213 nm to around 200 nm, a value very close to the 195 nm minimum observed for random coil peptides and commonly found for unfolded ptoteins (Fig. 1A).[33] Additionally, the maximum emission wavelength shows a red-shift from around 335 nm to 350-355 nm which corresponds to the maximum emission observed for tryptophan residues exposed to aqueous environments (Fig. 1C).[34] The HMQC spectrum of ^{13}C-methyl-Ala-TTR in the native state shows twelve peaks corresponding to the twelve alanine residues present in each TTR subunit (Fig. 2A). In the acid-unfolded form, those peaks merge into a single resonance reflecting the identical chemical environment sensed by the alanine residues (Fig. 2B). SEC-MALS assays were performed at pH 2 and more than 95 % of the total amount of protein eluted at 17 min in a peak corresponding to an apparent molecular mass of 16-18 kDa as calculated from the excess Rayleigh ratio data (Fig. S1). This value is slightly higher than the molecular mass of the TTR subunit (13.7 kDa) which may result from the less compact unfolded conformation of the protein.

TTR aggregation kinetics

The amyloidogenic potential of TTR arises from the balance between tetramer dissociation, monomer stability, and aggregation tendency.[3,25-27,35] To evaluate the

kinetics of TTR amyloid formation isolated from the tetramer dissociation step, aggregation was induced by the addition of 0.1 M NaCl to acid-unfolded TTR monomers.[28] The chloride ions shield the protein positive charges allowing for a conformational change and assembly of the monomers into oligomers and eventually fibrils. TTR aggregation kinetics assays were performed at protein concentrations ranging from 9.2 to 64 μM (as monomer) using different spectroscopic methods: CD, intrinsic TTR fluorescence, and ThT fluorescence. Upon NaCl addition, the minimum of the CD spectrum shifts from 200 to 213 nm, indicating that TTR acquires a mostly β-sheet conformation and the progressive increase in the intensity of the CD signal reflects the increase and progressive stabilization of the β-sheet conformation (Fig. 1A and 1B). Additionally, the fluorescence emission maximum shifts from 350-355 to around 335 nm reflecting the burial of tryptophan residues upon aggregation (Fig. 1C and 1D). In addition, we have employed the widely used ThT dye, a probe which fluorescence is known to increase upon interaction with amyloid fibrils[9], to follow the TTR aggregation reaction (Fig. 1E and 1F). ThT was added to the sample before salt addition since it has previously been proven that the presence of ThT does not affect TTR aggregation.[30] The increase in ThT fluorescence immediately after NaCl addition indicates that the initial steps of TTR oligomerization produce oligomers with amyloid-like tinctorial properties (Fig. 1F).

The data obtained with different spectroscopic techniques and at different protein concentrations could not be fitted to a single exponential function but all kinetic traces could be well fitted to a sum of two exponential functions, for a mechanism involving two first-order consecutive steps. However, the rate constant for the first step showed a very strong dependence on protein concentration (Fig. S2) which indicates that higher order reactions must be considered. Hence, kinetic traces were numerically integrated to a model comprising an initial second order step and a subsequent unimolecular step (Scheme 1 and Equation 1) (Fig. 1B, 1D and 1F).

$$U \xrightarrow{k_1} O \xrightarrow{k_2} FA$$ Scheme 1

$$\begin{cases} \dfrac{\partial[U]}{\partial t} = -\, k_1[U]^2 \\ \dfrac{\partial[O]}{\partial t} = k_1[U]^2 - k_2[O] \\ \dfrac{\partial[FA]}{\partial t} = k_2[O] \end{cases} \qquad \text{Equation 1}$$

were U represents the acid-unfolded conformation of TTR, O represents intermediate oligomers and FA represents TTR fibrillar aggregates or small soluble fibrils.

Very good agreement was found between the rate constants obtained by the three techniques employed indicating that NaCl addition induces structural changes of the TTR acid-unfolded monomers producing oligomers with β-sheet conformation and amyloid-like nature (Fig. 3). The rate constants obtained from data fitting to model 1 were found to be concentration independent with values of, approximately, 24 $M^{-1}s^{-1}$ and 3 x 10^{-4} s^{-1} for k_1 and k_2, respectively. The rate constant of the first step is several orders of magnitude higher than the rate constant of the second step, at the protein concentrations tested, indicating that the growth step is the rate limiting one and hence, there is accumulation of intermediate species in the TTR oligomerization pathway. Identification of this intermediate oligomer was also obtained by SEC-MALS (see below).

Aggregation kinetics was also followed by NMR. Upon aggregation, the linewidth of the HMQC NMR signals increases and eventually the signals disappear in the baseline. Thus, the decrease of the ^{13}C-methyl-Ala-TTR signal with time was also used to monitor the kinetics of TTR oligomerization (Fig. 2C). As the protein concentration required to perform the NMR experiments is higher (244 μM) than that used in CD or fluorescence experiments and also due to the lower time resolution of these assays, it is not possible to retrieve accurate information for the rate constants. However, assuming that the height of the initial NMR signal is equal to that of the ^{13}C-methyl-Ala peak before the NaCl addition, and by fitting the NMR data to a sum of two exponential functions we obtained two rate constants in the 10^{-3} to 10^{-5} s^{-1} order of magnitude. Notably, the first rate constant is in very good agreement with the k_2 constant obtained from the analysis of the CD and fluorescence data (Fig. 3) demonstrating that the decrease in NMR signal reports TTR aggregation.

TTR aggregation mechanism

To get insight into the species accumulated during TTR oligomerization, SEC-MALS experiments were carried out (Fig. 4). This technique allows for the separation of the molecular species formed during protein aggregation and also the determination of their molecular mass and relative amount. At pH 2 and in the absence of NaCl, virtually all TTR eluted from the SEC column in a single peak corresponding to the unfolded monomers (Fig. S1). Upon NaCl addition, the intensity of the monomer peak decreases and new species start to elute (Fig. 4). The last peak elutes at around 19-20 min corresponding to a calculated molecular mass of 20 to 30 kDa, a value higher than the 13.7 kDa of the TTR monomer suggesting that a mixture of monomers and dimers are eluted in this peak (Table 1). The elution of these species occurs later than the elution of the unfolded monomer (see above) indicating that their conformations are more compact. A second peak eluted from the SEC column with a retention time of 17 min corresponding to an apparent molecular mass between 80 and 140 kDa indicating that oligomers with 6 to 10 monomeric units are present in the reaction mixture (Table 1). This peak appears transiently being clearly visible in the chromatogram obtained 30 min after salt addition to the 9.2 μM TTR solution (Fig. 4A). At higher protein concentration these oligomers do not accumulate to high amounts because the aggregation reaction is faster but their elution from the column is also visible, specially at the earlier time points (Fig. 4B). As the reaction progresses, larger aggregates are formed eluting at shorter times or even within the column dead volume (11-12 min) (Table 1).

Transmission electron microscopy (TEM)

TTR aggregation was also evaluated by TEM (Fig. 5). Before NaCl addition, no visible structures were found in the TEM images (data not shown). However, 10 min after NaCl addition to acid-unfolded 9.2 μM TTR, small spherical aggregates are visible with a diameter of about 13 nm. As aggregation proceeds, these aggregates become more compact and, after 25 min of incubation, spherical structures with 10 nm diameter are observed. At longer time points (from hours to days), 30 to 90 nm length fibrils are visible with a diameter of 8 to 9 nm which is similar to the diameter observed for mature amyloid TTR fibrils.[36,37]

DISCUSSION

In this work, we have used several biophysical techniques to characterize the kinetics of TTR aggregation into amyloid fibrils. In order to simplify the study of TTR aggregation kinetics, we produced acid-unfolded monomeric TTR and triggered TTR amyloidogenesis by addition of 0.1 M NaCl. Upon extensive dialysis against 10 mM HCl, TTR disassembles and the monomers unfold as shown by the CD spectrum with a minimum at around 200 nm, corresponding to a protein with large amounts of random coil, and a fluorescence emission maximum at 350-355 nm, corresponding to the fluorescence characteristic of tryptophan residues exposed to aqueous solvent (Fig. 1).

We examined the kinetics of the initial steps of TTR aggregation by CD, intrinsic tryptophan fluorescence and also using the probe Thioflavin-T (ThT) that is known to interact with proteins with amyloid conformation. The use of these techniques allow the monitoring of TTR oligomerization from different approaches, namely, the increase in β-sheet conformation, the burial of tryptophan residues within aggregates and the appearence of amyloid structures, respectively. Additionally, while ThT assays give an indirect measure of protein aggregation, CD and tryptophan fluorescence monitor directly the conformational changes accompanying the TTR oligomerization reaction. The decrease in the volume of the single peak observed in the NMR [^{1}H-^{13}C]-HMQC spectrum of acid-unfolded TTR labelled with ^{13}C-methyl-Ala was also used to monitor TTR aggregation. The much higher concentration and lower time resolution of this experiment precluded the determination of the first rate constant of the aggregation reaction. However, it is remarkable that the first rate constant retrieved from the fitting of the NMR data to a sum of two exponential functions is excellent agreement with the first order rate constant (k_2) obtained from the adjustment of the CD and fluorescence data to the Scheme 1 model (Fig. 2 and 3). As was observed by TEM, after the initial steps of aggregation, growth continues during several days to yield mature fibrils and, probably, the second rate constant determined from the NMR assay may reflect this maturation process, however, further studies are required to confirm this hypothesis which is beyond the scope of this work.

Upon NaCl addition to the acid-unfolded TTR, there was an immediate variation of the signal detected by CD and tryptophan fluorescence and no lag-phase was observed in the aggregation kinetics, confirming that TTR aggregation is a downhill polymerization reaction as shown in other studies.[30,31] In addition, the fluorescence of ThT also increases immediately after NaCl addition revealing that the oligomeric species formed

in the first step of the aggregation reaction present already amyloid-like properties. The kinetic traces were only accurately fitted by a model comprising two steps with the first being second-order and the second being unimolecular (Fig. 1B, D and F). There is a very good agreement between the results obtained by the three techniques used indicating that tryptophan burial and conformational changes leading to the formation of amyloid β-sheet structures are simultaneous processes. The rate constant of the first step was found to be much larger than that of the second step revealing that the growth of the oligomers into fibrillar aggregates is the rate-limiting step (Fig. 3). As a consequence, transient accumulation of intermediate oligomeric species is expected and in fact confirmed by SEC-MALS experiments. Several mathematical models reported in the literature to analyze kinetic data of amyloid formation make assumptions only valid for the classic nucleation-growth reactions where the first step is much slower that the second one which is not the case for TTR amyloidogenesis.[1,2] Based on the fundamentals of crystal growth, the crystallization-like model (CLM) was recently proposed as a generic model useful to analyze sigmoidal (classic nucleation-growth reactions presenting a lag-phase) and hyperbolic (traces without lag-phase) kinetic data.[32] This simple model determines two parameters; one reports the magnitude of the growth step as a function of protein supersaturation (k_a) and the other the nucleation-to-growth magnitude (k_b). We used the CLM to analyze TTR kinetic traces but k_b, that should be concentration-independent, showed a linear correlation with the protein supersaturation. This is in accordance with the analysis that the authors performed with experimental data for M-TTR, a monomeric TTR variant, at different concentrations. To explain this linear relationship, the authors suggested that oligomers with different sizes were formed at different protein concentrations.[32] However, this is proved wrong in the case of wild-type TTR since SEC-MALS analysis showed that similar oligomeric species composed by 6 to 10 monomers are formed at 9.2 and 64 μM TTR concentrations. These oligomers are observed as small spherical aggregates with approximately 13 nm diameter in electron micrographs (Fig. 5A). Annular oligomers with a diameter of 16 nm showing octameric symmetry where identified by AFM in the first hours of TTR aggregation under acidic conditions (pH 3.6)[38] and small globular structures with 8 to 9 nm were observed in the early stages of aggregation in physiological buffer of some highly amyloidogenic TTR variants by TEM.[37] Hence, in spite of the different experimental conditions, small globular oligomers appear as intermediate species during TTR aggregation. In accordance with the results obtained

for other amyloid proteins, toxicity studies of TTR towards different cells found that fibrils or large aggregates were not toxic and that TTR cytotoxicity arises mainly from early, rapidly formed aggregates.[31,39] Hence, in the case of TTR amyloidoses, small oligomeric structures composed by approximately eight monomers seem to be the causative agent of cell toxicity. This raises a question to be further investigated relating the role of aggregation kinetics and the extent of accumulation of initial globular oligomers in the amyloidogenic potential of several variants of TTR.

EXPERIMENTAL

Materials

Sodium chloride, thioflavin-T (ThT), 2,2,3,3-d4-3-(trimethylsilyl)propionic acid 98 %D (TSP) and deuterium oxide 99.9 %D were purchased from Sigma Aldrich, hydrochloric acid (37 %) was from Merck and all other chemicals were of the highest commercially available purity.

Protein expression and purification

Recombinant human wild-type TTR was produced in a *Escherichia coli* expression system. The gene encoding TTR was cloned into the pET23a plasmid between NdeI and EcoRI restriction sites allowing the production of TTR with no fusion tags and the resulting construct was transformed into BL21 star *E. coli* cells (Invitrogen). After growth in Luria Broth medium up to an optical density at 600 nm of approximately 0.7, cells were washed with M9 salt solution and then ressuspended in M9 Minimal Medium with one fourth of the initial volume. One hour after medium exchange, the expression of TTR was induced with 1 mM IPTG and induction lasted 4 hours. For the production of ^{13}C-methyl-Ala TTR, M9 minimal medium was supplemented with ^{13}C-methyl-Ala at a concentration of 0.1 g/l. After cell harvesting and a freeze/thaw cycle, the cells were sonicated and the insoluble materials pelleted by centrifugation. The purification protocol comprised an initial fractionation by ammonium sulfate precipitation (TTR was collected from the soluble fraction at 55 % ammonium sulfate saturation, precipitated at 85 % saturation), followed by dialysis against 50 mM phosphate buffer pH 7.2. The protein solution was loaded onto an anionic exchange chromatography column (HiPrep 16/10 Q FastFlow column from GE Healthcare), equilibrated with the same buffer, and operating at a flow rate of 5 ml/mim. NaCl was used to elute the

proteins adsorbed to the matrix and TTR eluted at 300 mM NaCl. The purity of the sample was evaluated by SEC-MALS (see below) after dialysis to remove NaCl. If protein contaminants were observed, size exclusion chromatography (Hi Prep 16/60 Sephacryl S-200 High Resolution column) was carried out with the same buffer at a flow rate of 0.5 ml/min to isolate the TTR tetramer. Chromatographic steps were performed on an Akta Purifier UPC-900 equipment. SDS-PAGE electrophoresis and SEC-MALS were used to check TTR purity. TTR tetramer concentrations were determined spectrophotometrically at 280 nm using an extinction coefficient of 1.41 $mg^{-1}cm^{-1}$.[40]

Sample preparation

Native tetrameric TTR solutions were prepared by dialysis against 50 mM phosphate buffer, pH 7.2. Samples of acid-unfolded TTR at pH 2 were prepared by dialysis against 10 mM HCl for 96 hours at 4 °C in a Slide-A-Lyzer cassette (Thermo scientific) with a molecular weight cut off membrane of 3500 Da. TTR aggregation was induced by addition of NaCl to a final concentration of 0.1 M.[28] Aggregation assays were performed at 24 °C with TTR concentrations ranging from 9.2 to 64 μM (as monomer).

Circular dichroism spectroscopy (CD)

Far ultraviolet circular dichroism (CD) data was acquired on an Olis DSM 20 circular dichroism spectropolarimeter continuously purged with nitrogen, equipped with a Quantum Northwest CD 150 Temperature-Controller system and controlled by the Globalworks software. Scans were collected between 190 and 260 nm at 1 nm intervals. Depending on the protein concentration, cuvettes with a pathlength of 0.2, 1 or 2 mm were used. Three spectral scans with an integration time of 5 seconds per nm were averaged. Baselines with buffer were also acquired and subtracted from the raw CD data. Data is presented as mean residue molar ellipticity. Aggregation time course assays at 24 °C were monitored at 213 nm with an integration period of 6 seconds per point.

Intrinsic tryptophan fluorescence

Fluorescence experiments were preformed on a Varian Cary spectrofluorometer controlled by the Varian Cary Eclipse software version 1.1. Assays were carried out at 24 °C in 5 x 5 mm pathlength cuvettes with excitation and emission slits of 5 nm and

with a magnetic stirrer for agitation. Before NaCl addition and after the end of the aggregation reaction, emission scans were collected between 300 and 450 nm with an excitation wavelength of 290 nm. Protein aggregation kinetics was studied by monitoring the intrinsic tryptophan emission at 380 nm with an excitation wavelength of 290 nm and an integration time of 9 seconds per point.

Thioflavin-T (ThT) assay

Thioflavin-T (ThT) was used to probe amyloid formation. A freshly prepared stock solution of ThT (in 5 mM glycine-NaOH buffer, pH 9.0) was added to protein solutions in a final concentration of 10 μM. ThT emission was monitored at 485 nm with the excitation wavelength set at 450 nm and an integration time of 15 seconds. Assays were carried out at 24 °C in 5 x 5 mm pathlength cuvettes with excitation and emission slits of 5 nm and continuous agitation with a magnetic stirrer.[9] Spectra of ThT fluorescence were collected between 460 and 560 nm with an excitation wavelength of 450 nm.

Size exclusion chromatography (SEC) coupled to multi-angle light scattering (MALS) and UV absorption

Evaluation of TTR oligomerization state was also carried out by size exclusion chromatography (SEC) using a TSK Gel G300SW$_{XL}$ column (Tosoh Bioscience) connected to a P500 pump (Pharmacia) operating at a flow rate of 0.5 ml/min with filtered 10 mM HCl and 0.1 M NaCl, pH 2, at room temperature. The total amount of protein in each injection was approximately 0.4 μg (as monomer). Eluted fractions passed through a mini-DAWN TREOS (Wyatt Technology) multi-angle light scattering (MALS) detector and a UV/VIS-151 (Gilson) UV detector at 280 nm. The calibration of MALS to convert the signals measured to Rayleigh ratios was performed using HPLC grade toluene and the normalization of detector's signals relative to the 90 ° detector (normalization coefficient of 1) was carried out with bovine serum albumin according to the manufacture's manual. Analysis of the MALS chromatograms was performed using the Astra V software (Wyatt Technology).

Nuclear magnetic resonance (NMR)

TTR labelled with ^{13}C-methyl-Ala was prepared to a final concentration of approximately 244 μM (as monomer) in a solution containing 90 % H_2O /10 % D_2O

(v/v) and 3.6 mM of TSP. NMR measurements were performed on a Bruker Avance III spectrometer operating at a proton frequency of 400.133 MHz at 24 °C.

Two-dimensional [^{1}H-^{13}C]-HMQC experiments[41] were collected using the States-TPPI method in the indirect detected dimension.[42] Data were acquired with 2k complex points in t2 and 64 increments (16 scans each) in t1 using digital quadrature detection, a spectral width of 6410 Hz (16 ppm) in the direct dimension, and 4024 Hz (40 ppm) in the indirect dimension, and a recycle delay of 6 seconds. The water signal was suppressed using the standard presaturation method. The spectra were apodized with a QSINE window function in both dimensions and zero filled to 4k and 512 points in the direct and indirect dimensions respectively. All data were processed and analysed using the program Topspin v2.1 (Bruker).

Transmission electron microscopy (TEM)

At different time points, TTR aggregates were analyzed by transmission electron microscopy (TEM). Sample aliquots (5 µl) were adsorbed to carbon coated collodium film supported on 400-mesh copper grids for 1 min. The grids were negatively stained with 1 % uranyl acetate and visualized with a EM 902A Zeiss transmission electron microscope operating at 80 kV equipped with a Gatan SC1000 Orius CCD camera.

CONCLUSIONS

In this work we propose a mathematically simple two-step kinetic mechanism to analyse the aggregation kinetics of WT-TTR from acid-unfolded monomers. The model accommodates the protein concentration dependence of the aggregation reaction and it comprises an initial faster step leading to the formation of globular oligomers with 6 to 10 monomers and a second slower step leading to the formation of fibrils. This model may be used to evaluate the aggregation of other TTR variants and eventually to test if there is higher accumulation of toxic intermediates in more amyloidogenic mutants and if these arise from higher nucleation rates or decreased growth kinetics. The kinetic model proposed will also be useful to assess the effect of potential therapeutic agents against TTR amyloidoses on the protein aggregation pathway.

REFERENCES

1. M. Morris, M. A. Watzky and R.G. Finke, *Biochim. Biophys. Acta*, 2009, **1794**, 375.
2. J. P. Bernacki and R. M. Murphy, *Biophys. J.*, 2009, **96**, 2871.
3. R. M. M. Brito, A. M. Damas and M. J. S. Saraiva, *Curr. Med. Chem. - Immun. Endoc. & Metab. Agents*, 2003, **3**, 349.
4. F. Chiti and C. M. Dobson, *Annu. Rev. Biochem.*, 2006, **75**, 333.
5. T. Eichner and S. E. Radford, *Mol. Cell*, 2011, **43**, 8.
6. M. Sunde and C. Blake, *Adv. Protein Chem.*, 1997, **50**, 123.
7. L. C. Serpell, M. Sunde, M. D. Benson, G. A. Tennent, M. B. Pepys and P. E. Fraser, *J. Mol. Biol.*, 2000, **300**, 1033.
8. H. Puchtler, F. Sweat and M. Levine, *J. Histochem. Cytochem.*, 1962, **10**, 355.
9. H. LeVine III, *Protein Sci.*, 1993, **2**, 404.
10. W. G. Gosal, I. J. Morten, E. W. Hewitt, A. Smith, N. H. Thomson and S. E. Radford, *J. Mol. Biol.*, 2005, **351**, 850.
11. H. Toyama and J. S. Weissman, *Annu. Rev. Biochem.*, 2011, **80**, 557.
12. Y. Ando and M. Ueda, *Curr. Med. Chem.*, 2012, **19**, 2312.
13. P. Westermark, K. Sletten, B. Johansson and G. G. Cornwell, *Proc. Natl. Acad. Sci. USA.*, 1990, **87**, 2843.
14. M. J. M. Saraiva, S. Birken, P. P. Costa and D. S. Goodman, *J. Clin. Invest.*, 1984, **74**, 104.
15. M. D. Benson, *Trends Neurosci.*, 1989, **12**, 88.
16. R. Jacobson, R. D. Pastore, R. Yaghoubian, I. Kane, G. Gallo, F. S. Buck and J. N. Buxbaum, *N. Engl. J. Med.*, 1997, **336**, 466.
17. Y. Sekijima, P. Hammarstrom, M. Matsumura, Y. Shimizu, M. Iwata, T. Tokuda, S. Ikeda and J. W. Kelly, *Lab. In*Vest., 2003, **83**, 409.
18. S. Mitsuhashi, M. Yazaki, T. Tokuda, Y. Sekijima, Y. Washimi, Y. Shimizu, Y. Ando, M. D. Benson and S. Ikeda, *Amyloid*, 2005, **12**, 216.
19. L. H. Connors, A. Lim, T. Prokaeva, V. A. Roskens and C. E. Costello, *Amyloid*, 2003, **10**, 160.
20. J. A. Hamilton and M. D. Benson, *Cell. Mol. Life Sci.*, 2001, **58**, 1491.

21. C. Blake, M. J. Geisow, S. J. Oatley, B. Rerat and C. Rerat, *J. Mol. Biol.*, 1978, **121**, 339.

22. J. A. Hamilton, L. K. Steinrauf, B. C. Braden, J. Liepnieks, M. D. Benson, G. Holmgren, O. Sandgren and L. Steen, *J. Biol. Chem.*, 1993, **268**, 2416.

23. Y. Kanda, D. S. Goodman, R. E. Canfield and F. J. Morgan, *J. Biol. Chem.*, 1974, **249**, 6796.

24. Z. Lai, W. Colón and J. W. Kelly, *Biochemistry*, 1996, **35**, 6470.

25. Quintas, M. J. M. Saraiva and R. M. M. Brito, *J. Biol. Chem.*, 1999, **274**, 32943.

26. Quintas, D. C. Vaz, I. Cardoso, M. J. M. Saraiva and R. M. M. Brito, *J. Biol. Chem.*, 2001, **276**, 27207.

27. P. Hammarström, X. Jiang, A. R. Hurshman, E. T. Powers and J. W. Kelly, *Proc. Natl. Acad. Sci. USA*, 2002, **99**, 16427.

28. M. Lindgren, K. Sörgjerd and P. Hammarström, *Biophys. J.*, 2005, **88**, 4200.

29. S. M. Johnson, S. Connelly, C. Fearns, E. T. Powers and J. W. Kelly, *J. Mol. Biol.*, 2012, **421**, 185.

30. A. R. Hurshman, J. T. White, E. T. Powers and J. W. Kelly, *Biochemistry*, 2004, **43**, 7365.

31. K. Sörgjerd, T. Klingstedt, M. Lindgren, K. Kågedal and P. Hammarström, *Biochem. Biophys. Res. Commun.*, 2008, **377**, 1072.

32. R. Crespo, F. A. Rocha, A. M. Damas and P. M. Martins, *J. Biol. Chem.*, 2012, **287**, 30585.

33. S. M. Kelly, T. J. Jess and N. C. Price, *Biochim. Biophys. Acta*, 2005, **1751**, 119.

34. T. Q. Faria, J. C. Lima, M. Bastos, A. L. Maçanita and H. Santos, *J. Biol. Chem.*, 2004, **279**, 48680.

35. A. Quintas, M. J. M. Saraiva and R. M. M. Brito, *FEBS Lett.*, 1997, **418**, 297.

36. L. C. Serpell, M. Sunde, P. E. Fraser, P. K. Luther, E. P. Morris, O. Sangren, E. Lundgren and C. C. Blake, *J. Mol. Biol.*, 1995, **254**, 113.

37. K. Andersson, A. Olofsson, E. H. Nielsen, S. E. Svehag and E. Lundgren, *Biochem. Biophys. Res. Comm.*, 2002, **294**, 309.

38. R. H. Pires, Á. Karsai, M. J. Saraiva, A. M Damas and M. S. Z. Kellermayer, *PLoSOne*, 2012, **7**, e44992.

39. N. Reixach, S. Deechongkit, X. Jiang, J. W. Kelly and J. N. Buxbaum, *Proc. Natl. Acad. Sci. USA*, 2004, **101**, 2817.

40. A. Raz and D. S. Goodman, *J. Biol. Chem.*, 1969, **244**, 3230.

41. A. Bax, R. H. Griffey and B. L. Hawkins, *J. Magn. Reson.*, 1983, **55**, 301.

42. D. Marion, M. Ikura, R. Tschudin and A. Bax, *J. Magn. Reson.*, 1969, **85**, 393.

ACKNOWLEDGMENTS

This work was funded by ERDF – European Regional Development Fund through the COMPETE Programme (Operational Programme for Competitiveness) and by National Funds through FCT – Fundação para a Ciência e a Tecnologia (Portuguese Foundation for Science and Technology) and grants PTDC/QUI-QUI/122900/2010, Pest-OE/QUI/UI0313/2014 (Coimbra Chemistry Centre) and Pest-C/SAU/LA0001/2013-2014 (Center for Neuroscience and Cell Biology). NMR data was collected at the UC-NMR facility, supported in part by grants REEQ/481/QUI/2006, RECI/QEQ-QFI/0168/2012 and PT-NMR. CSHJ acknowledges the FCT SFRH/BD/43896/2008 fellowship.

Table 1. Molecular mass (kDa) of the species eluted from the SEC column at different times after salt addition.

TTR concentration (μM)		**9.2**							
Aggregation time		0 h	0.5 h	2 h	4 h	8 h	16 h	20 h	24 h
Elution time (min)	19-20	26.8	29.3	26.0	33.3	33.3	45.2	27.8	41.2
	16-18	119.2	104.2	100.1	113.9	136.9	133.6	124.1	151.8
	11-12	-	181.7	188.5	215.6	351.1	443.9	517.1	622.2
Monomers per oligomer*		9	8	7	8	10	10	9	11
TTR concentration (μM)		**64**							
Aggregation time		0 min	2 min	10 min	30 min	60 min	2 h	5 h	
Elution time (min)	19-20	21.6	22.2	20.2	31.9	26.6	25.9	22.4	
	16-18	72.2	83.2	73.0	74.2	100.7	117.4	134.9	
	11-12	-	150.0	254.0	347.7	391.8	558.5	637.7	
Monomers per oligomer*		5	6	5	5	7	9	10	

* Monomers per oligomer values were calculated by dividing the mass of the oligomer (species eluted at 16-18 min) by the mass of the TTR monomer (13.7 kDa).

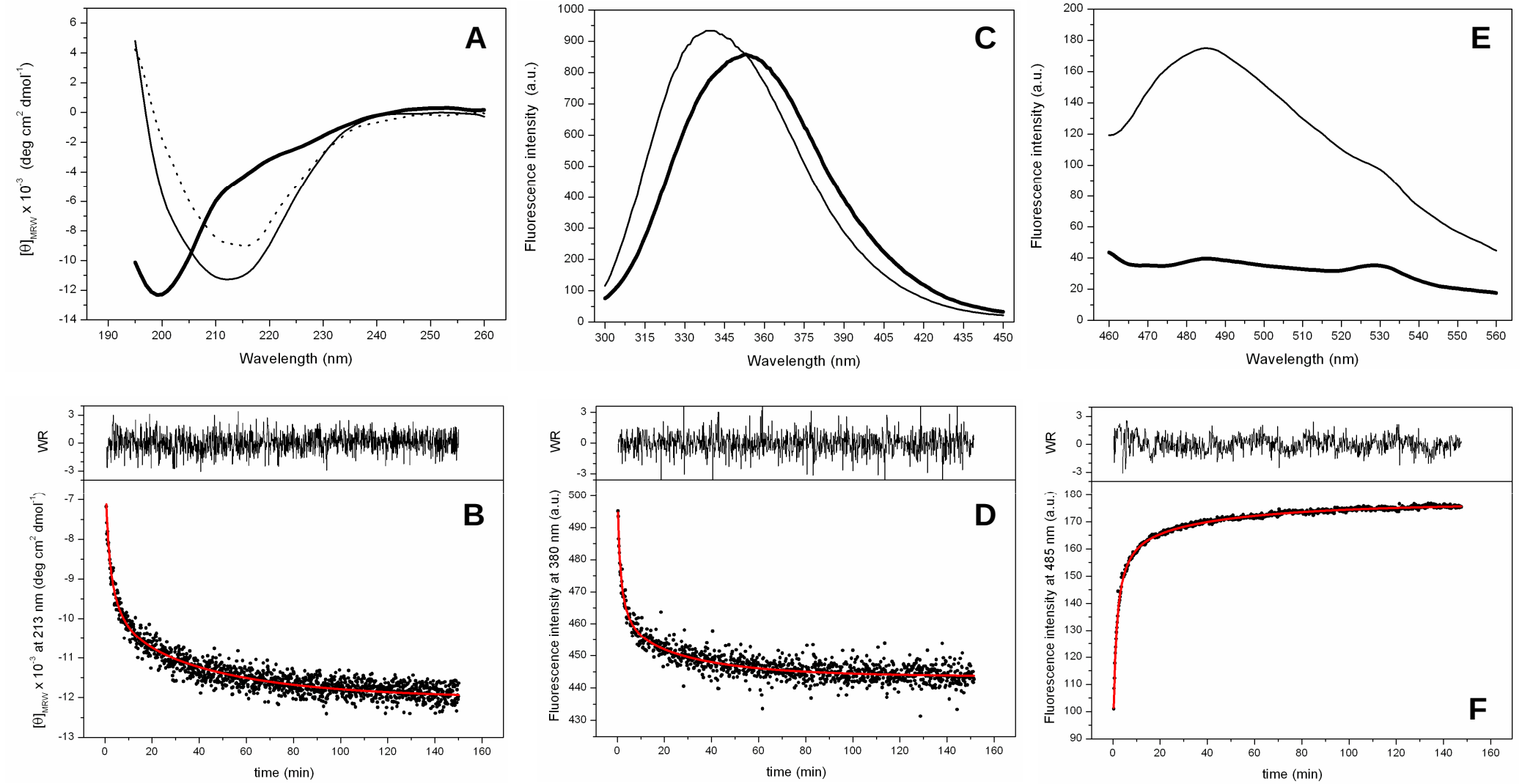

Fig. 1. TTR conformational changes (A, C, E) and aggregation kinetics (B, D, F) as monitored by CD (A, B), intrinsic tryptophan fluorescence (C, D) and ThT fluorescence (E, F). Protein concentrations were approximately 64 µM (as monomer). (A, C, E) Thick solid line: spectra of the acid-unfolded TTR; thin dashed line: spectrum obtained 15 min after NaCl addition; thin solid line: spectra obtained at the end of the kinetic assay; (B, D, F) Kinetic traces after NaCl addition monitored by CD (B), tryptophan emission (D) and ThT fluorescence (F); Red line: fit of the data to the Scheme 1 model; WR: weighted residuals.

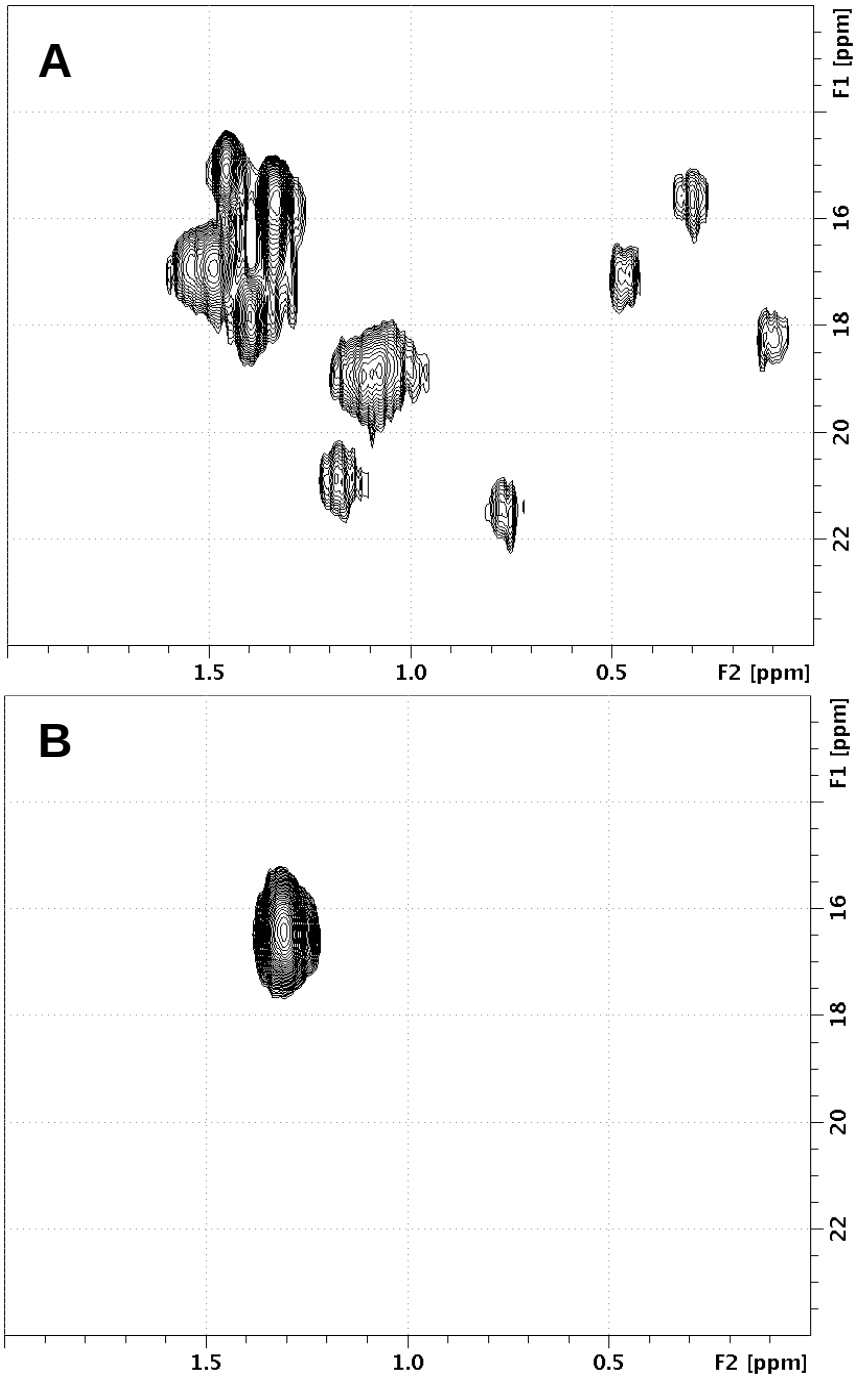

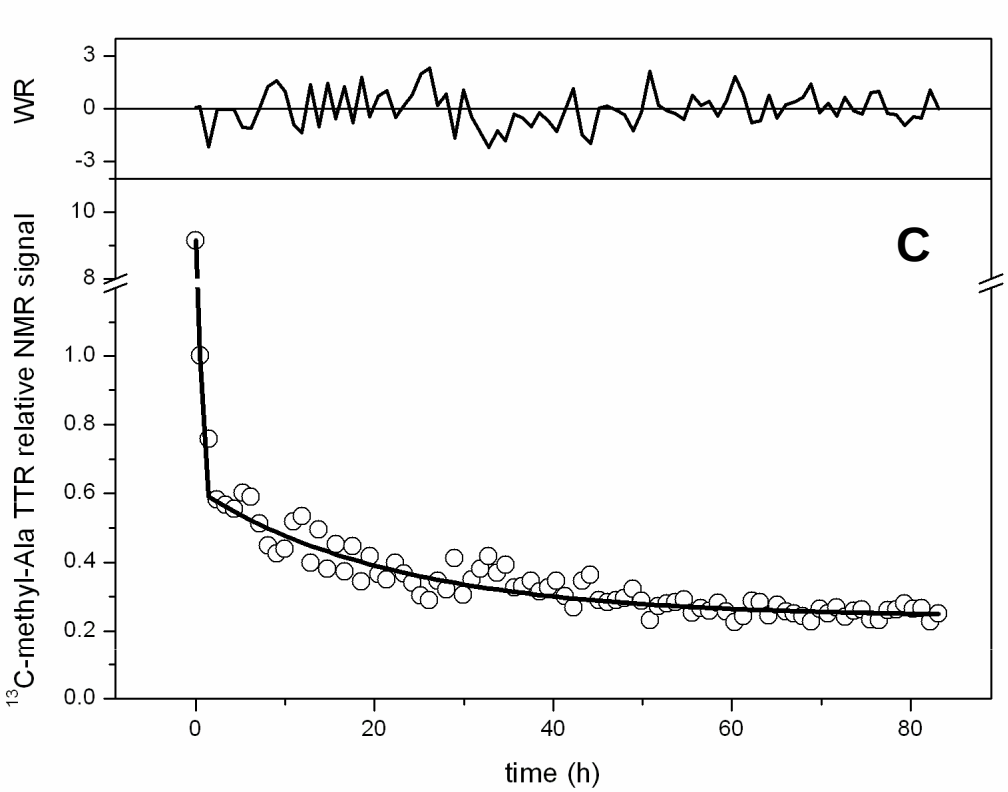

Fig 2. Protein aggregation followed by [^{1}H-^{13}C] HMQC NMR spectra of TTR labelled with ^{13}C-methyl-Ala. [^{1}H-^{13}C] HMQC NMR spectrum of native TTR at pH 7 (A) and acid-unfolded TTR at pH 2 (B). (C) Variation of the signal volume relative to a known reference after addition of 0.1 M NaCl. The line represents the fit of the data to a biexponential function with k_1 = 1.8 x 10^{-3} s^{-1} and k_2 = 1.3 x 10^{-5} s^{-1}. TTR concentration was approximately 244 µM (as monomer). WR represent the weighted residuals.

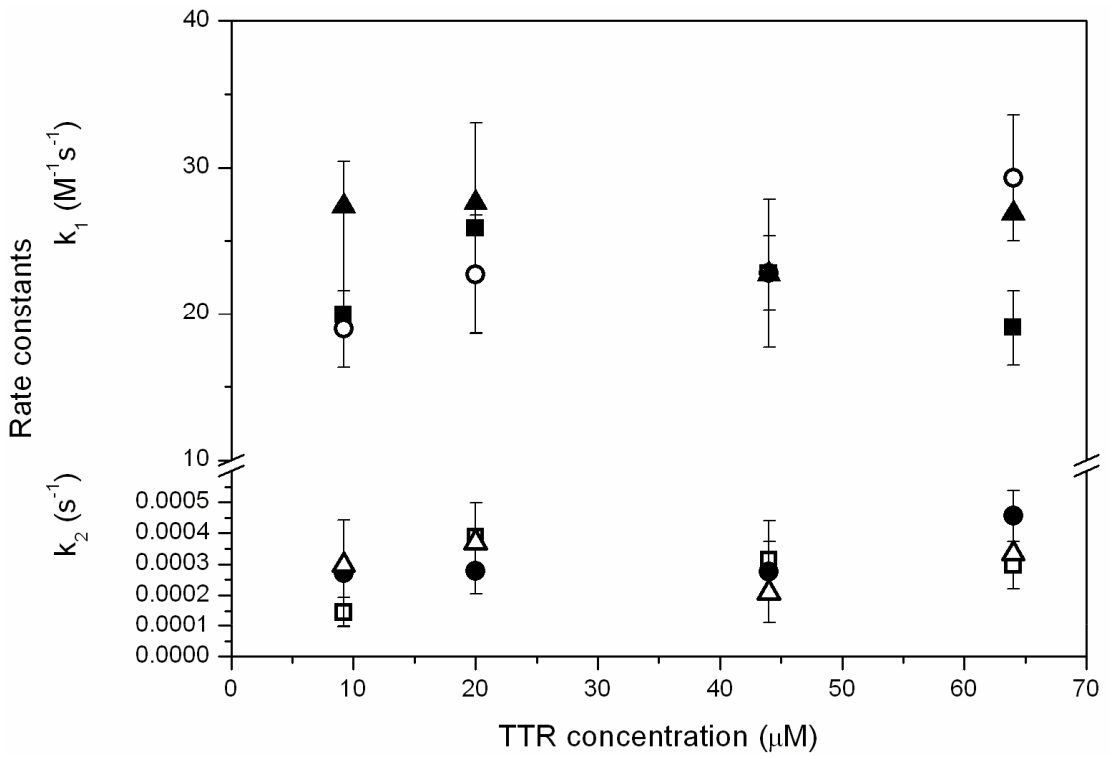

Fig. 3. Rate constants of TTR aggregation as a function of protein concentration (as monomer) obtained from the fitting of CD (squares), intrinsic tryptophan fluorescence (circles) and ThT fluorescence (triangles) data to equation 1 depicting the model in Scheme 1.

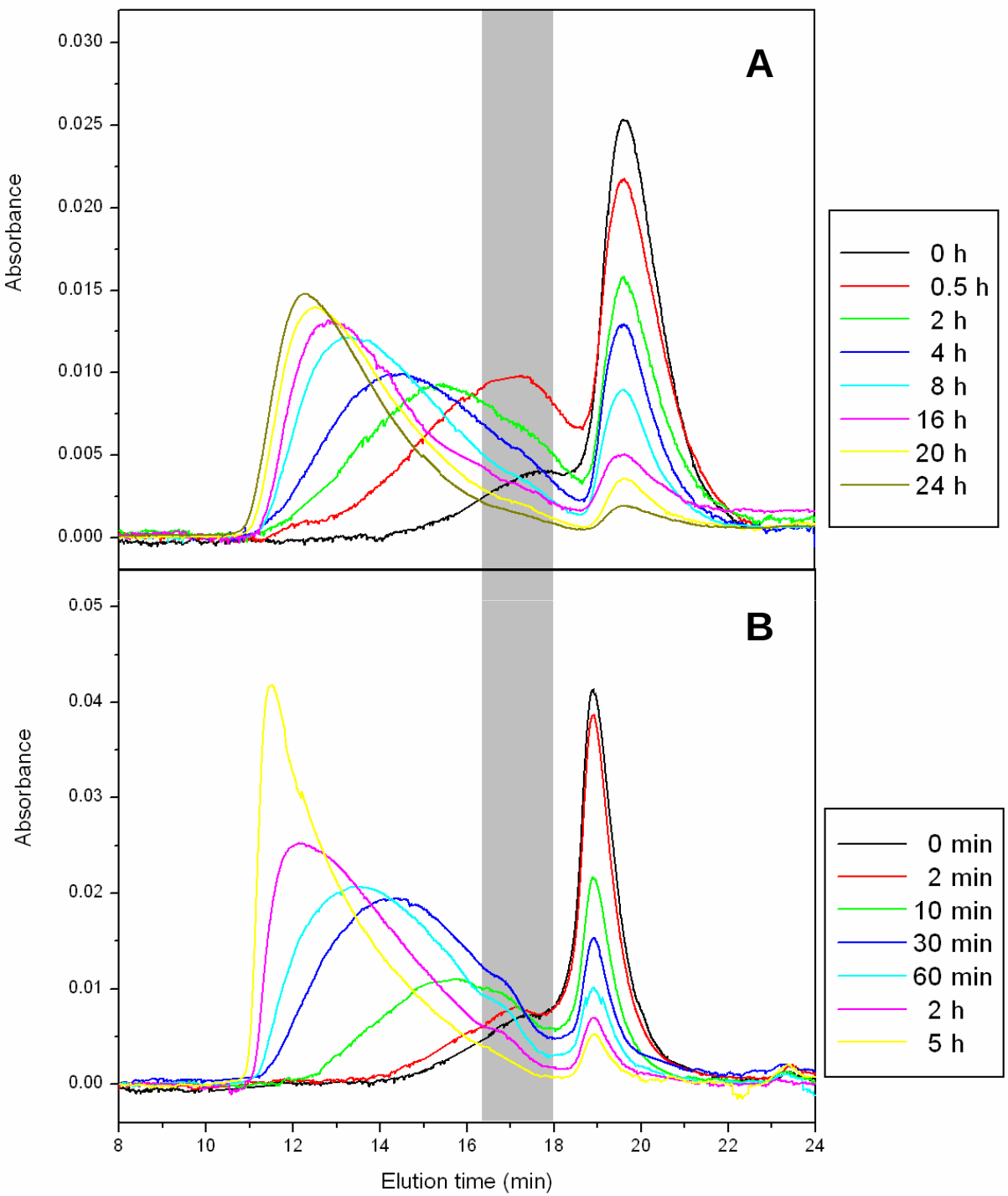

Fig. 4. Size exclusion chromatography coupled to multi-angle light scattering (MALS) and absorbance detection at different aggregation times and TTR concentrations of 9.2 µM (A) and 64 µM (B) (as monomer). Experiments were carried out at different incubation times after triggering TTR oligomerization as indicated in the figure. Grey areas highlight the transient accumulation of oligomeric intermediate species.

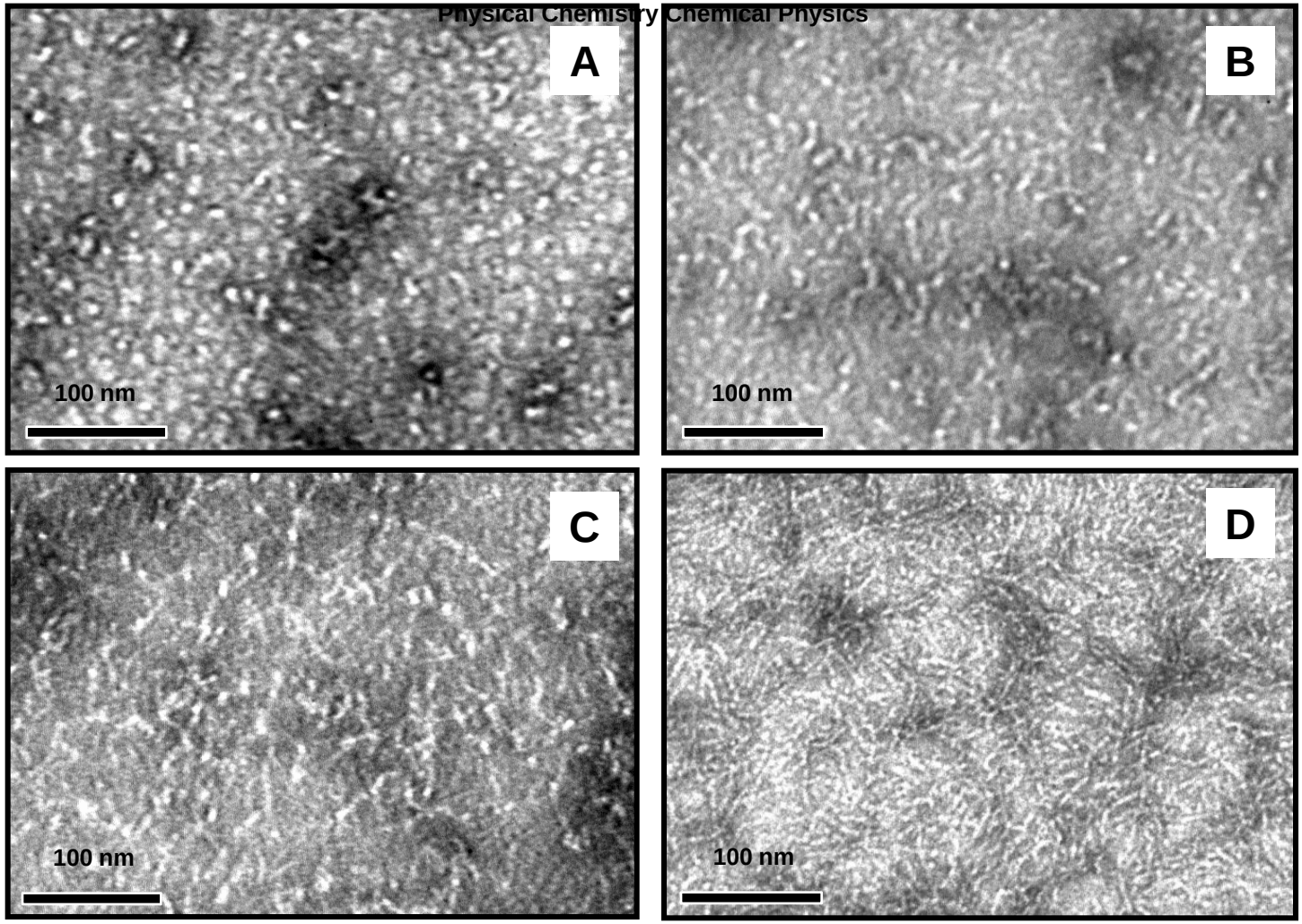

Fig. 5. Transmission electron microscopy images of TTR aggregates and fibrils. TTR aggregation was induced by incubation of acid-unfolded TTR monomers with 0.1 M NaCl for 10 min (A) and 3 hours (B) using a TTR concentration of 9.2 μM, 3 hours with 64 μM TTR (C) and more than 5 days at a concentration of 244 μM (D). TTR concentration is reported as monomer. The scale bar represents 100 nm.